

CELLULAR PHYSIOLOGICAL EFFECTS OF THE MV *KYOWA VIOLET* FUEL-OIL SPILL
ON THE HARD CORAL, *PORITES LOBATA*CRAIG A. DOWNS,[†] ROBERT H. RICHMOND,[‡] WOON JAYE MENDIOLA,[§] LUC ROUGÉE,^{||} and
GARY K. OSTRANDER,^{*‡||#}[†]Haereticus Environmental Laboratory, P.O. Box 92, Clifford, Virginia 24533, USA[‡]Kewalo Marine Laboratory, Pacific Biosciences Research Center, University of Hawaii at Manoa, 41 Ahui Street,
Honolulu, Hawaii 96813, USA[§]Marine Laboratory, University of Guam, UOG Station, Mangilao, Guam 96923, USA^{||}Department of Biology, Johns Hopkins University, 3400 North Charles Street, Baltimore, Maryland 21218, USA[#]Department of Comparative Medicine, Johns Hopkins University School of Medicine, Broadway Research Building,
Baltimore, Maryland 21205, USA

(Received 4 September 2005; Accepted 6 June 2006)

Abstract—The grounding of the Merchant Vessel (MV) *Kyowa Violet* on a coral reef near Yap, Federated States of Micronesia, in December 2002 resulted in the release of an estimated 55,000 to 80,000 gallons of intermediate fuel oil grade 180. The immediate impact was the widespread coating of mangroves and the intertidal zone along more than 8 km of coastline. Of greater concern, however, was the partitioning of the fuel oil in the water column, leading to chronic exposure of organisms in the ecosystem for a considerable period after the initial event. Herein, we report on our examination of one coral species, *Porites lobata*, nearly three months after the initial exposure. We investigated whether changes in cellular physiology were consistent with the pathological profile that results from the interaction of corals with polycyclic aromatic hydrocarbons, the principal constituent of fuel oil. Specifically, we document, to our knowledge for the first time, changes in the cellular physiological condition of an exposed coral population affected by a fuel-oil spill. We also provide evidence that the observed changes are consistent with a recent exposure to fuel oil, as evidenced by the presence of characteristic cellular lesions attributed to polycyclic aromatic hydrocarbons. Finally, our data support a model for a mechanistic relationship between the cellular pathological profile of the coral and a recent petroleum exposure, such as the MV *Kyowa Violet* fuel oil spill.

Keywords—Coral Oil spill Biomarker Cellular diagnostics

INTRODUCTION

The Merchant Vessel (MV) *Kyowa Violet* ran aground on a coral reef off of Colonia Harbor, Yap, Federated States of Micronesia, on December 26, 2002. Three separate areas of the reef adjacent to the Colonia Harbor entrance channel sustained physical damage from hull contact. An estimated 55,000 to 80,000 gallons of intermediate fuel oil grade 180 were released into the lagoon from the ruptured fuel tanks (A. Tafleichig, Chief, Yap Marine Resources Management Division, Colonia, Yap, Federated States of Micronesia, personal communication), resulting in extensive coating of mangroves and the intertidal coastal areas and affecting more than 8 km of coastline.

Evidence for direct exposure to a fuel-oil spill can be readily collected when visible fuel-oil residues are present, as in the MV *Kyowa Violet* spill [1] (<http://response.restoration.noaa.gov/>). Spill residues often are seen covering biological and geological structures along the interface of intertidal areas and surface waters (e.g., mangrove aerial roots and coastline). Less obvious, but often more damaging and more difficult to document, is damage to natural resources that arises from the invisible components of fuel oils that may partition in the water column, bind to dissolved organic matter, and/or be trapped in sediments. Such pollutants may become available for either chronic or pulsed exposures beyond the initial event [1].

Appropriate biological endpoints have yet to be fully ex-

ploited in documenting the exposure and impact of fuel-oil spills [2]. Acute mortality and gross changes in behavior (e.g., alpheid shrimp that normally inhabit goby burrows rapidly migrating to shore areas that are out of the water) can be used as cost-effective endpoints for both potential exposure and effect [3]. However, in the absence of acute mortality and morbidity, biological indicators have not been used successfully to identify delayed or sublethal effects in individuals that survived the initial exposure yet have compromised fitness as a result of the exposure [2]. The dilemma that investigators face concerning this type of event that damages natural resources can be reduced to two questions: Is there a sublethal or a submorbid effect, and is that biological change (effect) consistent with the nature of the exposure? This dilemma is further compounded by the fact that the biologically effective levels of many causative agents may be less than the detectable levels with the available instrumentation and methods (e.g., semi-permeable membrane devices and fluorescence spectroscopy), and even if a biological change is detected, it often is not understood in the context of its relationship to the nature of the exposure (e.g., inhibition of acetyl cholinesterase activity by polycyclic aromatic hydrocarbons [PAHs]) [4].

One method of resolving this dilemma is to determine if the changes in gross and cellular physiology are consistent with a pathological profile that results from the interaction of an organism with a defined stressor (e.g., aromatic hydrocarbon stress vs cadmium stress vs heat stress) [2,5]. A pathological profile is derived from reviewing a number of cellular and physiological responses or endpoints and determining

* To whom correspondence may be addressed (gko@hawaii.edu).
The current address of G.K. Ostrander is 2500 Campus Road, Hawaii Hall 211, University of Hawaii, Honolulu, HI 96822, USA.

whether the responses behave in a concordant manner; if they do, this should provide the investigator with a diagnostic interpretation. This diagnostic investigation cannot be based on a single endpoint, or on multiple endpoints that do not have an established mechanistic relationship [6]. This approach has not been adopted in environmental impact assessments, but it is a well-established methodology that has been successful in the fields of medicine and engineering and in criminal investigations that include forensic pathology [7]. Thus, the practice of environmental diagnostics applies diagnostic methods in answering the following questions: Is there a change because of a specific environmental phenomenon, what is the nature of that change, and can this change be associated with a specific causative stressor? Answering these three questions is essential in separating the effects of natural variation from human-induced impacts that result in an alleged event of natural resource damage [1,7–9].

The purpose of the present study was to determine whether the MV *Kyowa Violet* fuel-spill incident affected cellular physiological processes in corals exposed to the fuel. The goal of this investigation was to provide evidence for whether coral populations from the Ruul Causeway site exhibited a significantly different cellular biomarker profile from corals collected at the two reference reefs (South Ruul and Tamil) with similar ecological attributes. Moreover, if corals from the Ruul Causeway site did exhibit differences from those at the reference sites, we sought to determine whether these differences constituted a stressed condition for that population. These data then could formulate a mechanistic model that may explain the underlying pathological condition of the exposed corals and suggest possible causative agents that could produce the mechanism of pathology.

Here, we present evidence for the long-term effects of the MV *Kyowa Violet* fuel-oil spill on populations of the hard coral, *Porites lobata*, in the coastal intertidal zone of Yap Island. Our evidence documents a difference in cellular physiological condition in an exposed population of coral affected by the fuel-oil spill and provides a profile of that change that is consistent with exposure to fuel oil. We also document the presence of characteristic cellular lesions attributed to PAHs, which supports a model for a mechanistic relationship between the cellular pathological profile and a recent petroleum exposure, such as the MV *Kyowa Violet* fuel-oil spill.

MATERIALS AND METHODS

Sample collection

Porites lobata samples were collected at a depth of 1.5 m at the spill-impacted site (Ruul Causeway site, Yap, Federated States of Micronesia) and two non-fuel affected reference sites (Tamil and South Ruul, Yap, Federated States of Micronesia) in March 2003 (Fig. 1). Biopsy plugs (1.5 cm) were collected ($n = 10$) from each site. The plugs were placed in a Falcon tube (Fisher Scientific, Fair Lawn, NJ, USA), immediately frozen in liquid nitrogen, and stored at -80°C until analysis.

Enzyme-linked immunosorbent assay analysis

Samples were assayed according to methods adapted from Downs [6]. *Porites* biopsy disks were ground while frozen to a fine powder in a prechilled mortar and pestle using liquid nitrogen. Approximately 100 μl of frozen sample powder was placed in locking, 1.8-ml microcentrifuge tubes along with 1,400 μl of a denaturing buffer consisting of 2% sodium dodecyl sulfate (SDS), 50 mM Tris-HCl (pH 7.8), 15 mM dithiothreitol, 10 mM ethylenediaminetetra-acetate (EDTA), 3% polyvinylpyrrolidone (w/v), 0.005 mM salicylic acid,

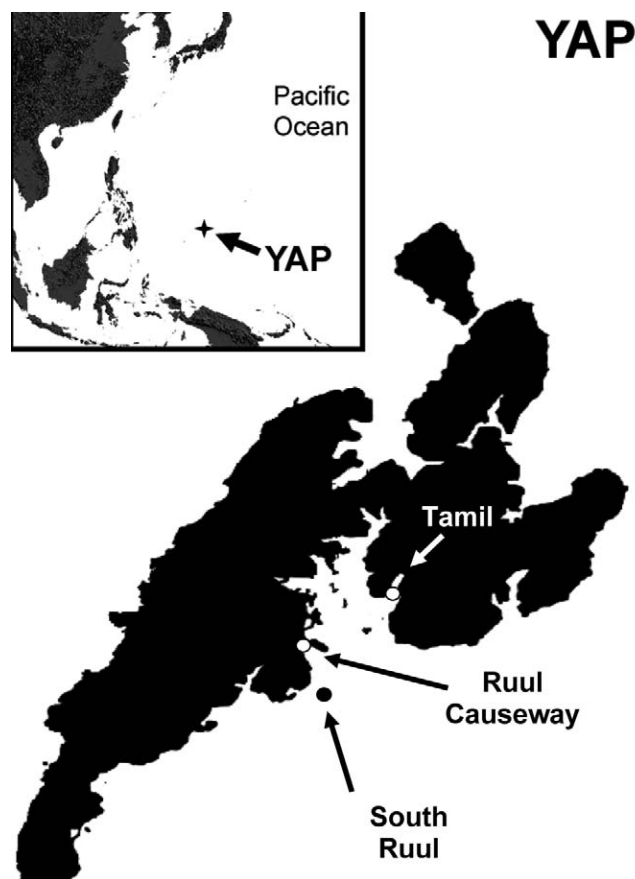


Fig. 1. Collections sites on the island of Yap, Federated States of Micronesia. Coral samples were collected from three sites along the coast of Yap. The fuel spill-affected site is designated as Ruul Causeway. Coral samples from two reference sites were collected: One site south of the spill (South Ruul), and one site north of the spill (Tamil).

0.001% (v/v) dimethyl sulfoxide, 0.01 mM 4-(2-aminoethyl)-benzenesulfonyl fluoride, 0.04 mM bestatin, 0.001 E-64, 2 mM phenylmethylsulfonyl fluoride, 2 mM benzamide, 5 μM α -amino-caproic acid, and 1 μg 100 pepstatin A^{-1} . Samples were vortexed for 15 s, heated at 93°C for 6 min with occasional vortexing, and then incubated at 25°C for 10 min. Samples were centrifuged (13,500 g for 8–10 min), and the middle-phase supernatant was aspirated and placed into a new tube [6]. The sample supernatant was subjected to a protein concentration assay according to the method described by Ghosh et al. [10].

One-dimensional SDS-polyacrylamide gel electrophoresis (PAGE) and Western blot analysis were used to optimize the separation of target proteins and to validate the use of specific antibodies for *P. lobata* protein extracts [9]. Total soluble protein (15–40 μg) from three randomly prepared samples was electrophoresed in a 12.5% SDS-PAGE preparative gel containing 0.001 M Tris(2-carboxyethyl) phosphine (neutral pH) until the bromophenol blue dye front was near the bottom of the gel. All gels were blotted onto polyvinylidene difluoride (PVDF) membranes (Millipore, Hercules, CA, USA) using a wet-transfer system. The membranes were blocked in 5% non-fat dry milk and assayed with a primary antibody for 1 h at 4°C . The blots were then washed four times in Tris-buffered saline and incubated in a 1:30,000 dilution of horseradish peroxidase-conjugated goat anti-rabbit secondary antibody solution (Jackson ImmunoResearch Laboratories, Westport, PA, USA) for 1 h at 4°C . Blots were washed again four times in

Tris-buffered saline solution and developed using an enhanced chemiluminescence solution (New England Nuclear, Shelton, CT, USA) and a Genegnome luminescent charge-coupled device camera documentation system (Syngene, Frederick, MD, USA). To characterize potential artifacts resulting from antibody nonspecific cross-reactivity, blots were overdeveloped for at least 7 min. Calibration using a quantitative standard showed that 0.05 attomole of target protein can be detected at this level of sensitivity.

Once validated, antibodies and samples were optimized for enzyme-linked immunosorbent assay (ELISA) using 384-well microplates in an $8 \times 6 \times 4$ factorial design [11] and were assayed using a Beckman Coulter Biomek 2000 (Promega, Madison, WI, USA). Sample extracts were assayed using the following antibodies from Enviro (Winchester, VA, USA): Cnidarian anti-heat shock protein 60 (AB-1508), cnidarian anti-heat shock protein 70 (AB-Hsp70-1517), cnidarian anti-heat shock protein 90 (AB-Hsp90-1685), cnidarian anti-manganese superoxide dismutase (AB-1976), cnidarian anti-copper/zinc superoxide dismutase (AB-SOD-1516), cnidarian anti-glutathione peroxidase (AB-GPX-1433), cnidarian anti-small heat shock protein (AB-H105), cnidarian anti-ferrochelatase (AB-FC-1939), cnidarian anti-cytochrome P450 6-class homologue (AB-C6-2), cnidarian anti-metallothionein (AB-MM-10843), cnidarian anti-heme oxygenase-1 (AB-HO-1944), anti-ubiquitin (AB-U100), and anti-multidrug resistant protein (AB-MDR4inv). All samples were assayed in triplicate; intraspecific variation of less than 8% was achieved throughout the 384 wells of each microplate. A calibrant relevant to a given antibody was plated in sextuplicate on each respective plate assayed to construct an eight-point calibration curve.

Measurement of benzo[a]pyrene-7,8-dihydrodiol-9,10-epoxide adducted to protein

Benzo[a]pyrene-7,8-dihydrodiol-9,10-epoxide (BPDE) was obtained from the National Cancer Institute Chemical Carcinogen Repository (Kansas City, MO, USA). The BPDE was dissolved in a 24:1 ethanol:tetrahydrofuran solution. Two-hundred milligrams of purified bovine serum albumin were added to a 0.5 mg BPDE/ml ethanol:tetrahydrofuran solution, and the mixture was incubated under stirring in the dark for 16 h at room temperature. The BPDE solution was then dialyzed using a 10,000-MW cutoff dialyzer cassette (Pierce, Rockford, IL, USA) in a 50 mM Tris (pH 7.4) buffer. The ratio of BPDE to albumin was determined using a modified method as described by Lee and Santella [12]. The anti-BPDE monoclonal antibody was obtained from Trevigen (4360-MC-100; Gaithersburg, MD, USA). A 32-fold serial dilution of the BPDE-albumin bound to a PVDF membrane was assayed with the anti-BPDE monoclonal antibody to determine the linear range of the calibrant standards. An eightfold serial dilution of 2,976 to 22 pmol of BPDE-albumin was determined to be a linear range for this calibrant. One microgram of coral total soluble protein per well was loaded (in triplicate) onto a 96-well dot blotter (Bio-Rad, Hercules, CA, USA) with PVDF as the solid-phase membrane. After transfer of the sample to the membrane, the membrane was blocked in 5% nonfat dry milk and assayed with the anti-BPDE monoclonal antibody for 1 h. The blot was then washed four times in a Tris-saline buffer and then incubated in a 1:30,000 dilution of horseradish peroxidase-conjugated secondary antibody solution for 1 h at 4°C. The blot was washed again four times in a Tris-saline buffer and developed using a chemiluminescent reporter system described above. To ensure a minimum of nonspecific cross-reactivity, blots were developed for at least 3 min, which was saturation.

Final results were obtained from blots that were detected using a 25-s exposure.

Porphyrin concentration determination

A total of 150 μg of total soluble protein from sample supernatants were diluted in a solution containing Tris-HCl (pH 7.8) and 5 mM EDTA to a volume of 300 μl . Next, 100- μl microliter aliquots of each sample were dispensed in triplicate into a black, clear-bottom, Corning 96-well microtiter plate (VWR Labshop, Batavia, IL, USA). Then, 100 μl of 3 N HCl were added to each well, and the samples were incubated for 30 min at room temperature in the dark. Uroporphyrin standards were obtained from Porphyrin Products (Logan, UT, USA) and diluted using an eight-point calibrant standard curve from 0 to 1,000 pmol of uroporphyrin. These calibrant dilutions were plated in triplicate on each microtiter plate to be assayed. A fluorescence signal was detected using a FL800 series fluorescent/luminescent microplate reader (Bio-Tek Instruments, Winooski, VT, USA) with the excitation filter set for 405 nm and the emission filter set for 610 nm.

Statistical analyses

Planned (a priori) and unplanned (a posteriori or post hoc) comparison tests were used in the present study [6,13]. Data were tested for normality using the Kolmogorov-Smirnov test (with Lilliefors' correction) and for equal variance using the Levene median test. If the data were normally distributed and homogeneous, a one-way analysis of variance (ANOVA) was employed. When data did not meet the homogeneity of variances requirement for one-way ANOVA, we used a Kruskal-Wallis one-way ANOVA on ranks. When significant differences were found among treatment means, we used the Tukey-Kramer honestly significant difference method, the Dunn's post hoc test, or the Holm-Sidak test as an exact α -level test to determine differences between each of the populations [13].

We used canonical correlation analysis (CCA) as a heuristic tool to illustrate how biomarkers could be used to discriminate among populations. This is a method of eigen analysis that reveals the basic relationships between two matrices [14]—in our case, those of the three populations and the biomarker data. The CCA provided an objective statistical tool for determining if populations are significantly different from one another using sets of cellular biomarkers that are indicative of a cellular process (e.g., protein metabolic condition and xenobiotic response) and of which biomarkers contributed to those differences. This analysis required combining data from all three populations into one matrix, which we did by expressing biomarker responses in a given population as a proportion of their mean levels. Two assumptions of CCA, that stressor gradients were both independent and linear, were constraints of the experimental design.

RESULTS

ELISA validation

Antibodies against cellular parameters did not exhibit significant nonspecific cross-reactivity (Fig. 2) and, hence, could be validly used in an ELISA format. All blots presented in Figure 2 are overexposed blots, which is a technique to characterize the potential of nonspecific cross-reactivity for the ELISA. The ELISA microplate readings are based on a 4-s exposure. The level of sensitivity between the Syngene Genegnome documentation system and the Bio-Tek microplate reader are approximately equal; hence, the nonspecific, faint bands are nondetectable by the microplate reader. All these antibodies were made against polypeptides that were designed

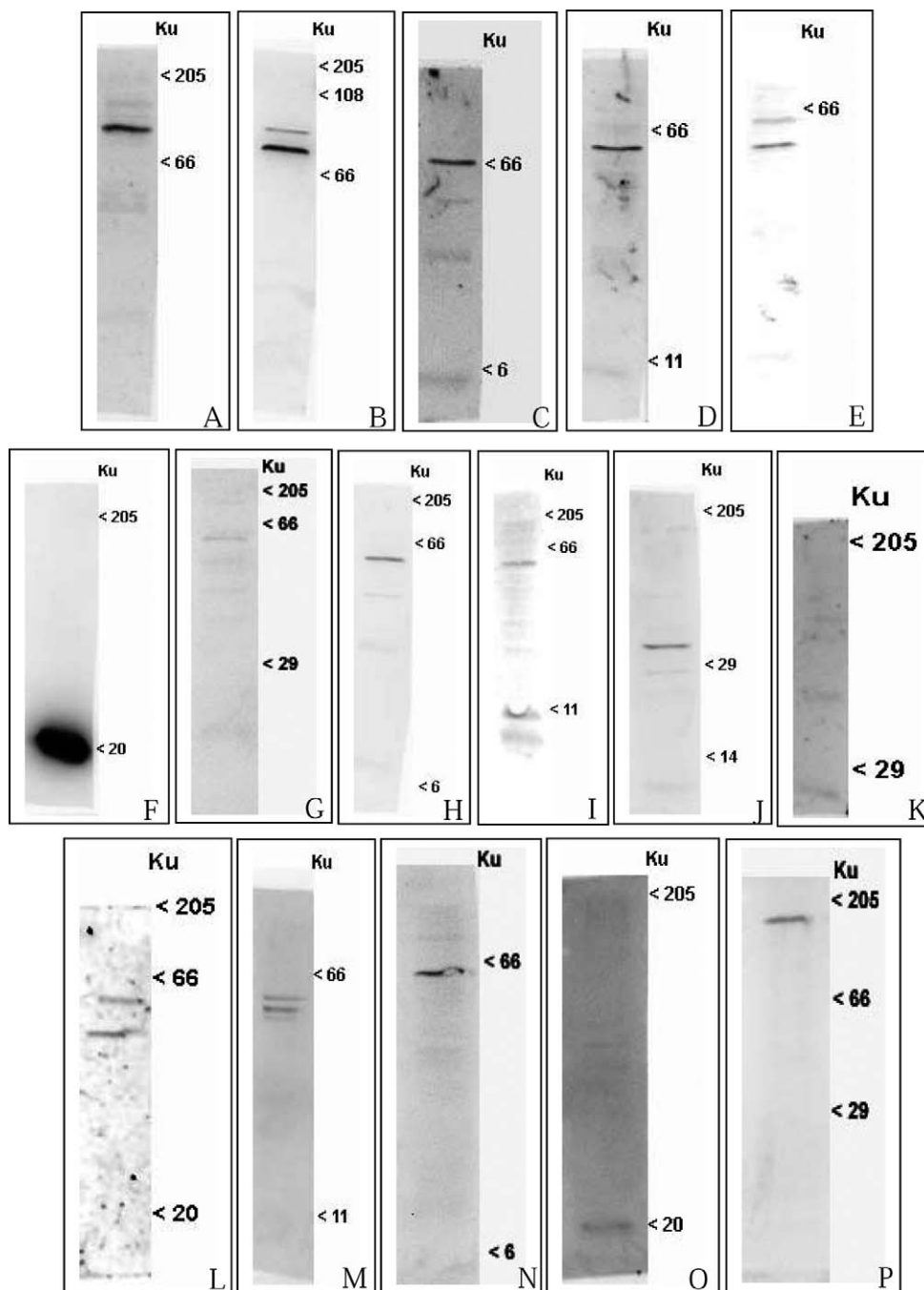


Fig. 2. Western blots for enzyme-linked immunosorbent assay validation (ELISA). Corals were homogenized and subjected to sodium dodecyl sulfate–polyacrylamide gel electrophoresis (total soluble protein, 5 μ g/lane) and Western blot analysis, and then assayed with polyclonal antibodies against the following parameters: (A) heat shock protein 90, (B) heat shock protein 70, (C) glucose-related protein 75 (Grp75), (D) heat shock protein 60, (E) ubiquitin ligase E2, (F) copper/zinc superoxide dismutase, (G) catalase, (H) DNA glycosylase (MutY), (I) protoporphyrinogen oxidase IX, (J) heme oxygenase-1, (K) small heat-shock proteins, (L) cytochrome P450 1-class, (M) cytochrome P450 2-class, (N) cytochrome P450 6-class, (O) glutathione-S-transferase, and (P) multixenobiotic resistant protein. Numbers along the sides of the blot indicate the position of the molecular migration rate marker, an estimator of a molecular weight. Ku = kilounits (Standard International designation).

based on unique, but evolutionarily conserved, protein domains for each target protein. The doublet cross-reactivity seen for heat shock protein 70 (Hsp70) in Figure 2B is the result of a cross-reaction to Hsp70a (slower-migrating band) and Hsp70b (faster-migrating band). Both proteins are independently regulated, which presents a caveat in the ELISA for Hsp70 homologues; in the ELISA, it cannot be distinguished whether one or both of the Hsp70 homologues are being induced. Figure 2E shows two bands that demonstrate both ubiquitin ligase E2 isoforms. Both homologues are independently

regulated, which again incurs the same type of caveat that is associated with Hsp70. Figure 2K is the blot for the small heat shock protein (sHsp). The monomer of this protein is found migrating faster than the 29-Ku marker. A second band is perceptible above the 29-Ku marker and is approximately 44 Ku; this is the homodimer of the sHsp. This protein readily undergoes oligomerization under cellular-denaturing conditions. The multimeric state is its natural form under protein-denaturing conditions and is known to maintain an oligomerized state under SDS-PAGE examination [6]. Doublet and trip-

Table 1. Biomarker expression^a

Cellular Parameter ^a	Ruul Causeway	Tamil	South Ruul
Protein Metabolic Conditions			
Hsp70 (cnidarian)	25.2 ± 18.5A	85.1 ± 27.7AB	87.7 ± 78.9B
Grp75 (cnidarian)	819.6 ± 561.3A	72.9 ± 33.9B	66.0 ± 60.7B
Hsp60 (cnidarian)	152.3 ± 111.3A	637.2 ± 530.7B	318.8 ± 125.0AB
Ubiquitin	275.0 ± 130.1A	423.4 ± 351.0A	295.0 ± 349.6A
Ubiquitin ligase E2	119.5 ± 68.2A	47.4 ± 29.5B	31.1 ± 12.1B
sHsp (cnidarian)	226.3 ± 44.4A	55.4 ± 48.6B	51.4 ± 74.1B
Oxidative Damage and Response			
Cu/Zn superoxide dismutase (cnidarian)	274.4 ± 71.7A	176.6 ± 115.1AB	146.8 ± 100.75B
Glutathione peroxidase-1 (cnidarian)	11.1 ± 4.8A	7.4 ± 3.6A	6.8 ± 5.2A
Catalase (cnidarian)	139.3 ± 41.8A	52.7 ± 15.1B	41.5 ± 30.2B
MutY	14.3 ± 10.8A	2.4 ± 0.6B	2.3 ± 0.3B
Porphyrin Metabolism			
Protoporphyrinogen oxidase IX	111.9 ± 10.6A	101.2 ± 14.5A	95.7 ± 13.8A
Ferrochelatase (cnidarian)	99.9 ± 51.5A	36.2 ± 16.1B	33.1 ± 25.5B
Heme oxygenase-1	86.7 ± 71.6A	31.4 ± 6.5B	33.8 ± 10.3B
Porphyrin (pmol/mg total soluble protein)	155.6 ± 31.1A	6 ± 4.1B	9 ± 2.9B
Xenobiotic Response			
Cytochrome P450 1-class	663.7 ± 242.3A	198.0 ± 52.0B	159.0 ± 73.1B
Cytochrome P450 2-class	67.3 ± 66.1A	17.5 ± 5.9B	16.7 ± 6.4B
Cytochrome P450 3-class	544.1 ± 94.8A	238.2 ± 169.4B	135.6 ± 120.5B
Cytochrome P450 6-class	137.9 ± 28.0A	106.7 ± 33.3AB	92.2 ± 28.1B
Glutathione-S-transferase (cnidarian)	266.9 ± 200.9A	121.5 ± 54.6AB	103.0 ± 66.4B
Multixenobiotic resistance protein (fmol/ng total soluble protein)	390.5 ± 47.0A	99.0 ± 33.3B	91.9 ± 48.4B
Glutathione-S-transferase (dinoflagellate)	190.4 ± 126.5A	87.2 ± 14.9B	70.8 ± 18.0B
Benz[<i>a</i>]pyrene-7,8-dihydrodiol-9,10-epoxide (pmol/mg total soluble protein)	22.8 ± 5.4A	BDL-B	BDL-B

^a Treatment means with different uppercase letters differed slightly at $\alpha=0.05$ using the three different posthoc tests described in *Materials and Methods*. All units, except where noted, are expressed as mol target analyte/ng total soluble protein. Indicated sites are all located at Yap, Federates States of Micronesia. Values are presented as the mean \pm standard error ($n = 10$). BDL = below detection limit; Hsp = heat shock protein; MutY = DNA glycolase MutY homologue; sHsp = small heat shock protein.

let banding patterns seen in Figures 2L–N are isohomologues for the cytochrome P450 (CYP 450) classes being examined.

ELISA results

The average coefficient of variation among the triplicates of each sample for each assay type was between 3.8 and 11.4%. The ELISA results are summarized in Table 1 and are divided into the Cellular Diagnostic categories of Protein Metabolic Condition, Oxidative Damage and Response, Porphyrin Metabolism, and Xenobiotic Response.

Levels of glucose-related protein 75 (Grp75), heat shock protein 60 (Hsp60), ubiquitin activase E1, and sHsp were significantly higher in corals from the Ruul Causeway site compared to those from the two reference sites (Table 1). The Hsp70 levels in samples from the Ruul Causeway were significantly different compared to levels in samples from the South Ruul site but not significantly different from levels in samples from the Tamil site. Ubiquitin levels were not significantly different among any of the sites.

Protoporphyrinogen oxidase IX levels were not significantly different among any of the sites, but levels of ferrochelatase, heme oxygenase-1, and porphyria species were all significantly higher in coral samples from the Ruul Causeway site compared to samples from the two reference sites (Table 1).

Corals from Ruul Causeway had significantly higher levels of catalase and MutY compared to levels of these same biomarkers in corals from both the Tamil and South Ruul sites. Levels of copper/zinc superoxide dismutase in the Ruul Causeway samples were significantly higher than levels found in corals from South Ruul, but they were not significantly different from levels in samples from the Tamil site. No signif-

icant difference for glutathione peroxidase in corals was found among any of the sites.

Levels of CYP450 1-class, 2-class, and 3-class as well as multixenobiotic resistance protein and cnidarian glutathione-S-transferase (GST-pi) were significantly higher in samples from the Ruul Causeway site compared to the values in samples from the two reference sites. Cytochrome P450 6-class and GST-pi levels in the Ruul Causeway samples were significantly higher compared to the South Ruul samples but not significantly different from the Tamil site samples. The BPDE conjugated to protein was detected in the Ruul Causeway samples, but the concentration was less than the level of detection in samples from both the Tamil and South Ruul sites.

DISCUSSION

Two principal criteria for investigating an event that damages natural resources are documentation of the putative stressor and documentation of the biological response [8,9,15–17]. A principal goal of an environmental investigation is to determine if an association exists between a biological response and a putative stressor as well as the nature of that association [6,8,9,15,16]. This is not a simple task, and it usually is a multistep endeavor. The first step in investigating such an event with a suspected causative agent is to document the range and composition of the exposure—in this case, measuring the PAH profile and degradation kinetics of the fuel that had spilled in the environment. The second step is describing the behavior of a biological response compared to a reference, which should include an assessment of biotic integrity (i.e., population, community, and ecosystem health) [6,10]. It is not enough to document only the changes in population- and community-level

behavior [6]. Evidence for a mechanism that links the putative stressor and the biological effect is required to establish a causal link between the biological response and the putative stressor [6,10]. This mechanism of pathology (effect) usually is embedded at a molecular or cellular level in the biological hierarchy [18]. The mode of action for oil/fuel exposure-induced stress occurs by altering metabolic pathways (e.g., enzyme inhibition) or perturbing cellular structures, such as membranes, the cytoskeleton, and genomic integrity [19]. Changes at the molecular and cellular level may then integrate into higher-order changes at the tissue, organism, population, and community levels [6].

Biomarkers are endpoints that reflect an aspect of biological function and integrity [6]. The purpose of employing any type of cellular biomarker is to facilitate an understanding of the mechanistic basis for the pathology exhibited by the organism/population as well as to document the biological response. Biomarkers, as used in the present study, have the added value of identifying problems or potential problems at sublethal levels, when mitigation efforts can be most effective. Like assembling a puzzle, the aim of evidence-based diagnostics is to piece together enough facts to allow the investigator to determine the cause and mechanistic mode of action that underlies the biological response [8]. An understanding of the altered cellular and physiological behavior, coupled with the knowledge of the changes that occurred in the population and community structures, should then provide clues to profile the potential causative factor. This knowledge can then be used to design a practical investigative protocol to document the presence of the causative agent. Once causation has been identified, an effective mitigation plan can be designed, and the effectiveness of the measures undertaken can be evaluated [7].

After an event causing environmental damage, there may be a line-up of suspected causative agents found in both the environment and the organism and, likely, a gradient of effects, both obvious and subtle. Detection of an adducted metabolite of a causative suspect, such as benzo[*a*]pyrene (BaP) adducted to DNA, RNA, or protein, decreases the probability of refuting the argument that a particular causative suspect (in this case, BaP and, perhaps, other PAHs) is not interacting with the organism/population [7]. In fact, such data are corroborative evidence for the mechanism of toxicity and a component in the profile for that suspected agent [8]. A dose-response laboratory experimental design using the suspected causative agent and the subject species can establish a model of toxicity for that stressor in the subject species [6–8]. Such a study cannot logically confirm that the mechanism of toxicity and the causative suspect is the actual mechanism responsible for the environmentally damaging event, but it can provide a measure of confidence for the cause-and-effect argument that is proposed for that event. It is crucial in that the evidence is appropriately used in a valid series of arguments that present a persuasive case linking the exposure event with adverse biological consequences [8,9,15,16].

Cellular diagnosis—Determining an effect and the nature of the effect

“Is there a difference in cellular physiological condition?” is best answered by Figure 3A. The centroids of all three populations do not overlap when almost all the biomarkers are included in the analysis. The fuel-affected Ruul Causeway site centroid is in significant spatial opposition to both reference site centroids. A significant difference exists between the two reference centroids, but this difference is not as severe as the difference with the impacted site. The nature of the differences

among these sites can be elucidated by examining specific categories of cellular physiology [6].

Protein metabolic condition. Protein metabolic condition is the cellular status of protein synthesis, protein maturation, and protein degradation. Changes in any of these processes are indicative of a significant change in cellular metabolism and homeostasis [6]. In the present study, we examined only five parameters of protein metabolic condition, but those were parameters for which changes in behavior are indicative of a wider system response. Heat shock protein 70 (Hsp70) is a cytosolic chaperonin, whereas Grp75 is the mitochondrial homologue. The cytosolic Hsp70 function is a crucial element in the maturation of newly made proteins to gain their active state. The Grp75 is essential in the maturation of newly imported proteins into the mitochondria. The ability to reassemble denatured proteins often is the most commonly recognized function of both Hsp70 and Grp75 [16]. Accumulation of these proteins can be interpreted as a shift in metabolic condition, but the direction of the shift is indeterminate by looking at Hsp70 or Grp75 alone. These markers must be examined in conjunction with other markers of protein metabolic condition [6]. Heat shock protein 60 is the major mitochondrial chaperonin and functions to mature nuclear-encoded, mitochondrial-imported proteins into their active state [16]. Elevation of this protein signifies a general shift in the protein metabolic condition of the mitochondria, which would implicate a possible change in the equilibria of many of the mitochondrial-associated metabolic pathways [17]. Ubiquitin could be considered to be the “death marker” for proteins; its conjugation to broken or no-longer-needed proteins marks these proteins for degradation [18]. Ubiquitin ligase E2 is the enzyme that is responsible for the actual conjugation catalysis event between ubiquitin and the target protein. Increases in ubiquitin ligase concentrations indicate that protein degradation processes have amplified [19].

Canonical correlation analysis indicated a significant difference in the protein metabolic condition of the Ruul Causeway samples compared to the samples from the other two reference sites (Fig. 3B). An understanding of this change in condition cannot come from examining changes in a single biomarker alone but, rather, must come from synthesizing responses from a suite of biomarkers functionally related and contributing to protein metabolic condition. Levels of Hsp70 in the Ruul Causeway corals were significantly lower than those expressed in corals from the South Ruul reference site, but they were not significantly different from levels found in the Tamil reference site corals, indicating that the Hsp70 stress response had been blunted at the Ruul Causeway site. Ubiquitin levels were not significantly different among all three sites, suggesting that at least for cytosolic protein metabolic condition, a significant shift toward protein degradation did not occur. Contrasted with the Hsp70 and ubiquitin data, the pattern of ubiquitin ligase E2 was significantly elevated in the Ruul Causeway samples compared to the corals from the two reference sites. This suggests that the corals at Ruul Causeway had an increased capacity to up-regulate protein degradation, as when the organism has had previous exposure to a protein-denaturing stress event but is not now experiencing such conditions. The Grp75 was significantly elevated in corals at the Ruul Causeway compared to samples from the two reference sites, indicating a shift in mitochondrial protein metabolic condition. The Hsp60 levels were not significantly different among corals from the three sites. The pattern of these two mitochondrial chaperonins suggests an increased demand for protein import, but the proteins being imported are not necessarily matrix-localized proteins, which are dependent on Hsp60 chap-

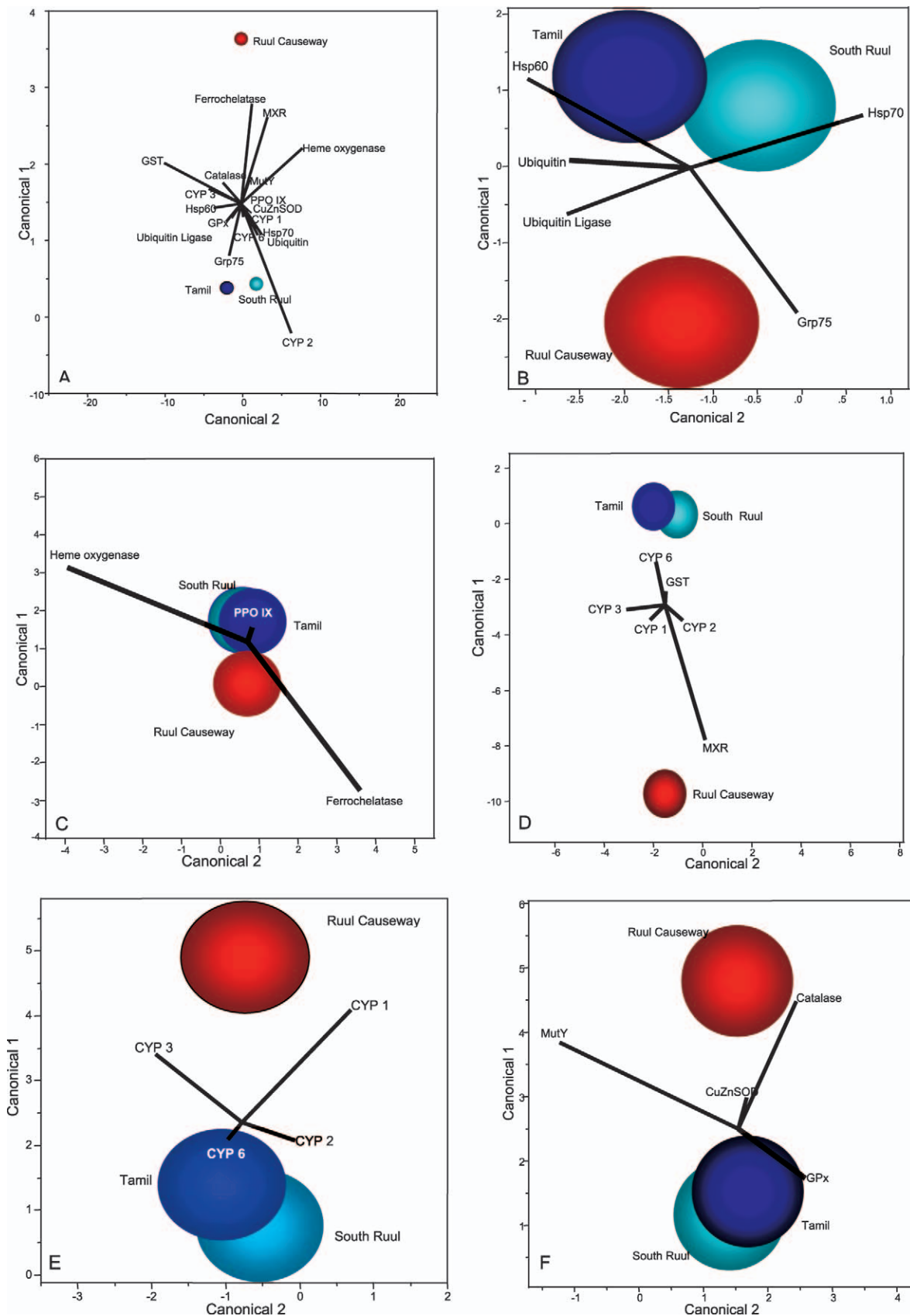


Fig. 3. Canonical correlation analysis. Original variants were biomarker levels expressed as a percentage of the control value in each treatment. Circles show the 95% confidence intervals around the distribution centroid of each stressor. Biplot rays radiating from the grand mean show directions of original biomarker responses in canonical space. Overlapping centroids indicate that those populations are not significantly different from one another, whereas nonoverlapping centroids indicate a difference. (A) Canonical centroid plot of almost all biomarkers combined. (B) Canonical centroid plot of Protein Metabolic Condition biomarkers. (C) Canonical centroid plot of Porphyrin Metabolism biomarkers. (D) Canonical centroid plot of Oxidative Stress biomarkers. (E) Canonical centroid plot of cytochrome P450 biomarkers. (F) Canonical centroid plot of Xenobiotic Response biomarkers. Cu/ZnSOD = copper/zinc superoxide dismutase; CYP 1 = cytochrome P450 1-class; CYP 2 = cytochrome P450 2-class; CYP 3 = cytochrome P450 3-class; CYP 6 = cytochrome P450 6-class; GPx = glutathione peroxidase; Grp75 = glucose-related protein 75; GST = glutathione-S-transferase; Hsp = heat shock protein; MutY = DNA glycosylase; MXR = multixenobiotic resistant protein; PPO IX = protoporphyrinogen oxidase IX.

eroning. Proteins that Grp75, but not Hsp60, chaperone include peripheral and integral membrane proteins, such as CYP 450 monooxygenase, and membrane transporter proteins, such as benzodiazepine-receptor proteins and proteins associated with sterol import (see, e.g., [20]). From the five protein metabolic condition parameters assayed, we interpret these findings to indicate that the difference in physiological condition in corals at the Ruul Causeway site from corals at the two reference sites is in response to an increase in mitochondrial protein chaperoning, especially of membrane-associated proteins and a poststress induction of the major cytosolic proteolytic pathway.

Porphyrim metabolism. Porphyrim metabolic condition was significantly altered in the corals from Ruul Causeway compared to those from the Tamil and South Ruul sites (Fig. 3C). This category includes enzymes responsible for the synthesis of porphyrins as well as enzymes responsible for the degradation of porphyrins. Shifts in the porphyrim metabolic equilibrium reflect a major shift in cellular metabolism as a whole [21]. Protoporphyrinogen oxidase IX catalyzes the second-to-last step of porphyrim production [22]. Levels of this protein were not significantly different among the three sites. Ferrochelatase is the last enzyme in porphyrim synthesis, and it inserts iron into the porphyrim ring to form heme [22]. Ferrochelatase levels were threefold higher in the Ruul Causeway corals compared to those from the two reference sites. Ferrochelatase often is the rate-limiting step for porphyrim production; hence, an increase in ferrochelatase indicates an increased demand in porphyrim [22]. Heme oxygenase-1 catalyzes the decomposition of heme to biliverdin, carbon monoxide, and ferrous iron [23]. Biliverdin is further catalyzed to bilirubin, which is a powerful lipophilic antioxidant [24]. The higher levels of heme oxygenase-1 in the samples from Ruul Causeway compared to those from the two reference sites indicate one of two things: A greater demand in the degradation of broken porphyrins, or a demand for higher lipophilic antioxidant defense capacity. The significant increase in porphyrim fluorescence in the Ruul Causeway samples compared to those from the reference sites supports the former hypothesis. Porphyrim fluorescence can occur when the metal ligand is removed from the porphyrim ring or when preporphyrim products accumulate as a result of porphyrim synthesis inhibition. Based on the data, the model that seems to be most probable is that free iron ions are being forcibly released from the heme proteins by some toxic compound, such as hydrogen peroxide, PAHs, or dioxin-like polychlorinated biphenyls [21].

Oxidative damage and response. A cell is able to withstand the adverse effects of oxidative stress based on its ability to suppress generation of reactive oxygen species, to neutralize reactive oxygen species once they are formed, and to repair the damage caused by a reactive oxygen species lesion to a cellular structure [24]. Canonical correlation analysis of the oxidative damage and response biomarkers indicated that corals from Ruul Causeway exhibited a significant oxidative stress condition compared to those from the two reference sites (Fig. 3F). Copper/zinc superoxide dismutase is a cytosolic protein that protects the cell from superoxide by catalyzing the superoxide into hydrogen peroxide [24]. Levels of this protein were not significantly different among the samples from the three sites, indicating that superoxide in the cytosol was not a significant factor for the coral cells. Glutathione peroxidase is another enzyme that scavenges superoxide by conjugating the reactive oxygen species with glutathione [24]. Levels of glutathione peroxidase were not significantly different among samples from the three sites, reinforcing the interpretation that superoxide was not a stress factor. Catalase is a cytosolic pro-

tein that converts hydrogen peroxide into water [24]. Levels of catalase were almost triple in samples from the Ruul Causeway compared to those from the reference sites. The source of hydrogen peroxide generation is unknown, but generation in either the mitochondria from the coral or its symbiotic dinoflagellates is possible [25,26]. The potential adverse effect of increased hydrogen peroxide include generation of hydroxyl radicals, which can result in protein, lipid, and DNA lesions as well as prompting the release of iron from heme molecules, resulting in damage to molecules such as cytochrome *c*, CYP 450 monooxygenases, or cellular death [27]. In turn, occurrence at the biochemical/subcellular level can affect cell survival, colony health, and susceptibility to coral bleaching [27]. These general effects need to be considered in light of the behavior of the porphyrim metabolism biomarker and the significant increase in the enzyme MutY. The MutY is an evolutionarily conserved DNA glycosylase that repairs certain DNA lesions caused by reactive oxygen [28]. Significant elevation of this protein in samples from the Ruul Causeway site compared to those from the reference sites indicates that some level of DNA oxidative damage is occurring or has recently occurred. Elevation of MutY and catalase indicates that corals from Ruul Causeway are experiencing or have recently experienced oxidative stress [25,27].

Xenobiotic response. Cells can regulate and expel potentially harmful xenobiotics through a three-phase process. In phase 1, xenobiotics undergo an enzymatically catalyzed reaction that introduces a polar group into the xenobiotic's molecular composition, such as a hydroxyl (-OH), carboxyl (-COOH), thiol (-SH), or an amino (-NH₂) group (for review, see [29]). Some of these modified xenobiotics result in a toxic species or enhanced toxicity compared to the parent compound. Enzymes responsible for such reactions include the superfamily of CYP 450s, the flavin-containing monooxygenases, and a host of esterases. In phase 2, these new polar metabolites are conjugated with endogenous substrates, such as sulfates, acetates, glutathione, and glucuronides. Enzymes of phase II include the family of glutathione-S-transferases, sulfotransferases, and uridine diphosphoglucuronosyltransferases [29]. These new water-soluble products can now be managed by the cell for transport to lysosomes for further metabolism, sequestered into lysosomal-like structures for containment, or excreted from the cell through active diffusion transporters, such as the adenosine triphosphate-binding cassette transporters (e.g., multidrug resistance protein-1) [30]. In the context of cellular economics, it is important to consider the energy and resource demands to up-regulate any of the components in this three-phase system. Any shift in this subcellular Xenobiotic Response system will exact a demand on other subcellular systems, such as Protein Metabolic Condition, Porphyrim Synthesis, Oxidative Defense, and Cellular Redox Capacity.

The CYP 450 superfamily of enzymes are membrane-bound hemoproteins that generally localize to microsomes, the endoplasmic reticulum, and mitochondria, where they catalyze the oxidation of a wide array of substrates [29,30]. Animals contain at least 50 isoforms of CYP 450 that are crucial components in pathways such as steroid metabolism, synthesis of lipid biofactors, and phase-1 toxification and detoxification [31]. Nomenclature of the CYP 450s is based on the level of homology. The CYP 450s with more than 40% amino acid identity are grouped into the same family, and members with 60% amino acid identity are grouped into the same subfamily. In the present study, we used antibodies that were specific to the family of CYP 450 but could not differentiate between subfamily members. For example, the antibody for CYP 450

6-class can detect only CYP 450 6-class homologues, which include members such as CYP 450 6A, 6B, 6D, and 6F, but the antibody cannot detect CYP 450s from the 1- to 4-classes [32,33]. Different species of CYP 450s from different families can catalyze the same substrate, but many of the CYP 450 families are differentially regulated and respond independently to xenobiotics. For example, many members of the CYP 450 1-class will hyperaccumulate in response to PAH exposure, whereas some members of the CYP 450 6-class will hyperaccumulate in response to pyrethroid exposure [32].

Canonical correlation analysis indicated a significant difference in CYP 450 profiles between corals from the Ruul Causeway site and those from the two reference sites (Fig. 3E). Levels of CYP 450 1-class, 2-class, and 3-class were significantly higher in samples from Ruul Causeway compared to the samples from the Tamil and South Ruul sites. Observed CYP 450 1-class induction suggests that the corals at Ruul Causeway were responding to an aromatic hydrocarbon exposure, which includes petrogenic and pyrogenic PAHs as well as biogenic aromatics, including sterols and polyphenols. The CYP 450 2-class and 3-class induction in the Ruul Causeway samples can occur by exposure to a wide range of hormonal, pheromonal, and xenobiotic substances, especially those with chlorinated side chains. For example, CYP 450 2-class monooxygenase can be induced by ethanol, carbon tetrachloride, and polychlorinated biphenyl congeners. The CYP 450 6-class is an invertebrate subfamily of CYP 450s that is known to oxidize and be up-regulated by pesticides, such as aldrin, dieldrin, diazinon, chlorpyrifos, deltamethrin, and a wide range of pyrethroid compounds [32]. Its lack of induction in the Ruul Causeway corals suggests that the factor affecting these corals is not similar to this category of compounds.

Glutathione-S-transferase is a multifamily enzyme that conjugates glutathione to exogenous and endogenous electrophilic toxic metabolites, such as benz[a]pyrene diol epoxide, 4-hydroxy-2-nonenal, and a wide range of phase-1 metabolized biocides (e.g., endosulfan and atrazine) [29]. In the coral samples analyzed, this GST species was not significantly different among sites. This behavior is consistent with the literature as well as with the described environment of these three sites in that GST-pi is not modulated by BaP and other PAH species [34]. The dinoflagellate GST was detected using an antibody made against a conserved domain found mostly in the plant GST-phi family. This enzyme is up-regulated by a number of xenobiotics, including PAHs, chemical fasteners (i.e., adhesives), and sulfonated aromatic herbicides, suggesting that both the corals and their dinoflagellate symbionts were responding to a xenobiotic [35].

Multixenobiotic resistance protein is an adenosine triphosphate-binding cassette transporter that exports glutathione-conjugated compounds out of the cell [30]. When compared to the other phase-1 and -2 biomarkers, up-regulation of this biomarker in the corals from the Ruul Causeway site strongly indicates that the organisms were detoxifying an endogenous or exogenously derived poison (Fig. 3D) [30].

Detection of PAH cellular lesions

Benzo[a]pyrene is a component of many different types of petrogenic and pyrogenic mixtures, such as fuels and oils. Several studies have demonstrated that a number of benthic marine invertebrates can clear BaP from their systems [36]. Benzo[a]pyrene is slightly toxic to the cell and can be removed by first activating it [37]. One general activation pathway of BaP is the oxidation across aromatic double bonds by the action of diverse CYP 450 monooxygenases. Another pathway is the formation of dihydrodiols via epoxide hydrolases. A

third pathway is the CYP 450 monooxygenase double action at the site of olefinic double bonds, resulting in the formation of highly reactive diol epoxides. Unfortunately, BPDE is a much more noxious toxicant than BaP and can readily adduct with DNA, RNA, and protein, creating cellular lesions that interfere with cellular processes and persist in the organism for some time [2,38]. The BPDE-adducted DNA is correlated with mutagenic and carcinogenic events. It is well known that BPDE can form adducts with specific amino acid residues of proteins, causing inactivation of enzymatic or functional activity [38]. Detection of BPDE-protein lesions in corals from Ruul Causeway is evidence of exposure to a petrogenic/pyrogenic source, supporting the argument that corals are responding to a PAH-based xenobiotic and are experiencing a level of toxicity from that source.

Model of cellular pathology

Corals from the Ruul Causeway site were experiencing an altered cellular physiological condition that is consistent with a response to a xenobiotic. Both the environmental contaminant analysis and the observed BPDE-protein cellular lesion support the argument that this xenobiotic is a PAH source. The cellular physiological diagnosis is consistent with previous and/or present exposure to this stressor. The presence of BPDE-protein, the high levels of CYP 450s, and antioxidative stress enzymes as well as the shift in protein metabolic condition strongly suggest a model proposed by Fucci et al. [39] that mixed-function oxidation centered on a CYP 450 monooxygenase (especially a CYP 450 1-class and 2-class) results in enzyme inactivation and increased protein turnover. This model suggests a mechanism for an increased rate of senescence or decreased cellular function, because many of the enzymes that are modified and inactivated by these oxidation reactions are the same enzymes that are significantly inactivated during senescence [24,39]. If this model is true in the case of the corals at the Ruul Causeway site, it would suggest that both corals at this locality would have a reduced reproductive fitness capacity, reduced immunocompetence capacity, and general reduction in individual fitness [2]. This oxidation model also would infer, with some supporting evidence, that the corals would have reduced genomic integrity, which in turn may directly affect the viability of offspring [24,39].

CONCLUSION

To our knowledge, the present study is the first to apply cellular diagnostic methods, commonly used in medicine and forensic pathology, to investigate whether sublethal and, perhaps, latent effects of a fuel-oil spill on a tropical coral reef adversely affected coral health [1]. The methodology used to investigate the putative damage consisted of measuring suites of cellular and physiological endpoints representing key metabolic processes in critical subcellular systems (i.e., protein metabolism, xenobiotic response, genomic integrity, and oxidative stress). These data created diagnostic profiles to resolve whether a damaging exposure had occurred and whether the exposure resulted in a pathological condition (i.e., resource injury). These profiles were then used to construct a mechanistic model to build a convincing argument to reasonably explain the cellular pathology and how it could be linked to a specific causative agent. The use of this environmental diagnostic approach in the present study provided compelling evidence that xenobiotics were present in the coral environment, that corals in proximity to the fuel-oil spill did experience an altered cellular physiological condition that was consistent with a xenobiotic exposure, and that exposures to com-

ponents from this spill were consistent with lesions found adducted to coral macromolecules (proteins).

Detection of an alleged event damaging natural resources sets in motion an investigative process that requires not only detection of an injury but also quantification of it and establishment of causation. Showing causation requires demonstrating the mechanism of toxicity for a given contaminant or set of toxicants, documenting exposure of the resource, and establishing an associated injury (pathology) to the resource. Exploiting the diagnostic method in investigations of natural resource damage associated with coral reefs opens new avenues for detecting injury, identifying causative agents, and constructing the links that are necessary to establish cause-and-effect relationships for use in coral reef resource management, protection, and litigation [40].

Acknowledgement—Research support was provided by a grant from the National Oceanic and Atmospheric Administration (NA04NOS4260204) and EnVirtue Biotechnologies. The authors gratefully acknowledge the assistance provided by the Yap Marine Resources Management Division, Marine Resources Pacific Consortium from the Department of the Interior, and Yimnang Golbuu.

REFERENCES

1. U.S. National Oceanographic and Atmospheric Administration. 2001. Oil spills in coral reefs: Planning and response consideration. U.S. National Oceanic and Atmospheric Administration, Washington, DC.
2. Downs CA, Shigenaka G, Fauth JE, Robinson CE, Huang A. 2002. Cellular physiological assessment of bivalves after chronic exposure to spilled *Exxon Valdez* crude oil using a novel molecular diagnostic biotechnology. *Environ Sci Technol* 36:2987–2993.
3. Fukuyama AK, Shigenaka G, Hoff RZ. 2000. Effects of residual *Exxon Valdez* oil on intertidal *Protothaca staminea*: Mortality, growth, and bioaccumulation of hydrocarbons in transplanted clams. *Mar Pollut Bull* 40:1042–1050.
4. Kang JJ, Fang HW. 1997. Polycyclic aromatic hydrocarbons inhibit the activity of acetylcholinesterase purified from electric eel. *Biochem Biophys Res Commun* 238:367–369.
5. Downs CA, Fauth JE, Woodley CM. 2001. Assessing the health of grass shrimp (*Palaeomonetes pugio*) exposed to natural and anthropogenic stressors: A molecular biomarker system. *Mar Biotechnol* 3:380–397.
6. Downs CA. 2005. Cellular Diagnostics and its application to aquatic and marine toxicology. In Ostrander G, ed, *Techniques in Aquatic Toxicology*. CRC, Boca Raton, FL, USA, pp 181–207.
7. Downs CA, Woodley CM, Richmond RH, Lanning LL, Owen R. 2005. Shifting the paradigm for coral reef ‘health’ assessment. *Mar Pollut Bull* 51:486–494.
8. U.S. Environmental Protection Agency. 2000. Stressor identification guidance document. EPA-822-B-00-025. Washington, DC.
9. Boehm PD, Galvani P, O'Donnell P. 1995. Scientific and legal conundrums in establishing injury and causation. In Stewart RB, ed, *Natural Resource Damages: A Legal, Economic, and Policy Analysis*. National Legal Center for the Public Interest, Washington, DC, pp 31–60.
10. Ghosh S, Gepstein S, Heikkila JJ, Dumbroff EB. 1988. Use of a scanning densitometer or an ELISA plate reader for measurement of nanogram amounts of protein in crude extracts from biological tissue. *Anal Biochem* 169:227–233.
11. Crowther JR. 2001. *The ELISA Guidebook*. Humana, Totowa, NJ, USA.
12. Lee BM, Santella RM. 1988. Quantitation of protein adducts as a marker of genotoxic exposure: Immunologic detection of benzo[a]pyrene-globin adducts in mice. *Carcinogenesis* 9:1773–1777.
13. Sokal RR, Rohlf FJ. 1995. *Biometry*. W.H. Freeman, New York, NY, USA, pp 451–499.
14. Gauch HGJ. 1985. *Multivariate Analysis in Community Ecology*. Cambridge University Press, New York, NY, USA.
15. Boehm PD, Douglas GS. 1995. Managing the NRDA process: Challenges in establishing causation and injury. In Stewart RB, ed, *Toxic Substances in Water Environments: Assessment and Control*. Water Environment Federation, Alexandria, VA, USA, pp 7-11 to 7-199.
16. Rougée L, Downs CA, Richmond RR, Ostrander GK. 2006. Alteration of normal cellular profiles in the scleractinian coral (*Pocillopora damicornis*) following laboratory exposure to fuel oil. *Environ Toxicol Chem* 25:3181–3187.
17. Ellis RJ. 1996. Stress proteins as molecular chaperones. In Van Eden W, Young DB, eds, *Stress Proteins in Medicine*. Marcel Dekker, New York, NY, USA, pp 1–26.
18. Papp E, Nardai G, Sti C, Csermely P. 2003. Molecular chaperones, stress proteins, and redox homeostasis. *Biofactors* 17:249–257.
19. Hershko A, Ciechanover A. 1998. The ubiquitin system. *Annu Rev Biochem* 67:425–479.
20. Shang F, Gong X, Taylor A. 1997. Activity of ubiquitin-dependent pathway in response to oxidative stress. *J Biol Chem* 272:23086–23093.
21. Marks GS. 1985. Exposure to toxic agents: The heme biosynthetic pathway and hemoproteins as indicator. *Crit Rev Toxicol* 15:151–179.
22. Dailey HA, Dailey TA, Wu CK, Medlock AE, Rose JP, Wang KF. 2000. Ferrochelatase at the millennium: Structures, mechanisms and [2Fe-2S] clusters. *Cell Mol Life Sci* 57:1909–1926.
23. Schwartzburd PM. 2001. Self-cytoprotection against stress: Feedback regulation of heme-dependent metabolism. *Cell Stress Chaperones* 6:1–5.
24. Halliwell B, Gutteridge JMC. 1999. *Free Radicals in Biology and Medicine*, 3rd ed. Oxford Science, Oxford, UK.
25. Downs CA, Mueller E, Phillips S, Fauth JE, Woodley CM. 2000. A molecular biomarker system for assessing the health of coral during heat stress. *Mar Biotechnol* 2:533–544.
26. de Zwart LL, Meerman JH, Commandeur JN, Vermeulen NP. 1999. Biomarkers of free radical damage applications in experimental animals and in humans. *Free Radical Biol Med* 126:202–226.
27. Downs CA, Fauth JE, Halas JC, Dustan P, Bemiss J, Woodley CM. 2002. Oxidative stress and coral bleaching. *Free Radic Biol Med* 33:533–543.
28. Pope MA, David SS. 2005. DNA damage recognition and repair by the marine MutY homologue. *DNA Repair* 4:91–102.
29. Jokanovic M. 2001. Biotransformation of organophosphorous compounds. *Toxicology* 166:139–160.
30. Borst P, Elferink RO. 2002. Mammalian ABC transporters in health and disease. *Annu Rev Biochem* 71:537–592.
31. Guengerich FP. 2004. Cytochrome P450: What have we learned and what are the future issues? *Drug Metab Rev* 36:159–197.
32. Scott JG, Wen Z. 2001. Cytochrome P450 of insects: The tip of the iceberg. *Pest Manag Sci* 57:958–967.
33. Dunkov BC, Guzov VM, Mocelin G, Shotkoski F, Brun A, Amichot M, French-Constant RH, Feyereisen R. 1997. The *Drosophila* cytochrome P450 gene Cyp6a2: Structure, localization, heterologous expression, and induction by phenobarbital. *DNA Cell Biol* 16:1345–1356.
34. Ketter B. 2001. A bird's eye view of the glutathione transferase field. *Chem-Biol Interact* 138:27–42.
35. Edwards R, Dixon DP, Walbot V. 2000. Plant glutathione-S-transferase: Enzymes with multiple functions in sickness and in health. *Trends Plant Sci* 5:193–198.
36. Ramakrishna NV, Gao F, Padmavathi NS, Cavalieri EL, Rogan EG, Cerny RL, Gross ML. 1992. Model adducts of benzo[a]pyrene and nucleosides formed from its radical cation and diol epoxide. *Chem Res Toxicol* 5:293–302.
37. Thakker DR, Yagi H, Akagi H, Koreeda M, Lu AH, Levin W, Wood AW, Conney AH, Jerina DM. 1997. Metabolism of benzo[a]pyrene. VI. Stereoselective metabolism of benzo[a]pyrene and benzo[a]pyrene 7,8-dihydrodiol to diol epoxides. *Chem-Biol Interact* 16:281–300.
38. Padros J, Pelletier E. 2000. In vivo formation of (+)-anti-benzo[a]pyrene diol-epoxide-plasma albumin adducts in fish. *Mar Environ Res* 50:347–351.
39. Fucci L, Oliver CN, Coon MJ, Stadtman ER. 1983. Inactivation of key metabolic enzymes by mixed-function oxidation reactions: Possible implication in protein turnover and aging. *Proc Natl Acad Sci U S A* 80:1521–1525.
40. Downs CA, Fauth JE, Robinson CE, Curry R, Lanzendorf B, Halas JC, Halas J, Woodley CM. 2005. Cellular diagnostics and coral health: Declining coral health in the Florida keys. *Mar Pollut Bull* 51:558–569.